Development 127, 5439-5448 (2000)
Printed in Great Britain © The Company of Biologists Limited 2000
DEV3305

Dosage requirement and allelic expression of *PAX6* during lens placode formation

Catherine D. van Raamsdonk and Shirley M. Tilghman*

Howard Hughes Medical Institute and Department of Molecular Biology, Princeton University, Princeton NJ 08544, USA
*Author for correspondence (e-mail: stilghman@molbio.princeton.edu

Accepted 29 September; published on WWW 14 November 2000

SUMMARY

***Pax6* is a member of the mammalian *Pax* transcription factor family. Many of the *Pax* genes display semi-dominant loss-of-function heterozygous phenotypes, yet the underlying cause for this dosage requirement is not known. Mice heterozygous for *Pax6* mutations exhibit small eyes (*Sey*) and in embryos the most obvious defect is a small lens. We have studied lens development in *Pax6*$^{Sey\text{-}1Neu}$/+ embryos to understand the basis of the haploinsufficiency. The formation of the lens pre-placode appears to be unaffected in heterozygotes, as deduced from the number of cells, the mitotic index, the amount of apoptosis and the expression of SOX2 and *Pax6* in the pre-placode. However, the formation of the lens placode is delayed. The cells at the edge of the lens cup fail to express N-cadherin and undergo apoptosis and the lens fails to detach completely from the surface ectoderm. After formation, the lens, which has 50% of the cells found in wild-type embryos, grows at a rate that is indistinguishable from wild type. We rule out the possibility that monoallelic expression of *Pax6* at the time of lens placode formation accounts for the 50% reduction in cell number by showing that expression of *Pax6* is biallelic in the lens placode and optic vesicle. We propose instead that a critical threshold of PAX6 protein is required for lens placode formation and that the time in development at which this level is reached is delayed in heterozygotes.**

Key words: *Pax6*, Lens placode, Haplo-insufficiency, Lens stalk, biallelism

INTRODUCTION

The nine mammalian *Pax* genes encode a family of transcription factors that contain paired box DNA binding domains, and function in developmental control. The *Pax* genes have diverse tissue-specific expression patterns, and homozygous mutations in the majority of them result in specific developmental defects (Mansouri et al., 1999). A curious feature of this family is that many *Pax* genes exhibit an unusual gene dosage requirement. Loss-of-function heterozygous mutations in *Pax1*, *Pax2*, *Pax3*, *Pax6*, *Pax8*, and possibly *Pax9* cause semi-dominant phenotypes in either the mouse or human, or both (Epstein et al., 1991; Hill et al., 1991; Ton et al., 1991; Baldwin et al., 1992; Hanson et al., 1994; Keller et al., 1994; Sanyanusin et al., 1995; Macchia et al., 1998; Wilm et al., 1998; Stockton et al., 2000). Frequently the affected tissue in the heterozygous mutants is reduced in size, and either more severely disrupted or missing altogether in homozygotes. The dosage requirement is also evident from the developmental defects caused by over-expression of *Pax2* and *Pax6* in transgenic mice (Dressler et al., 1993; Schedl et al., 1996).

The molecular basis for the *Pax* gene dosage requirement is not known, although it has generally been assumed that the protein products of these genes act within a concentration range that is sensitive to twofold changes. Alternatively it has been suggested, based on the monoallelic expression of *Pax5* (Nutt et al., 1999), that haplo-insufficiency could be explained if heterozygous cells activated either the wild-type or mutant allele, but not both (Nutt and Busslinger, 1999). This would generate a heterogeneous population of wild-type and null cells in *Pax* heterozygous animals. In normal animals, this process could serve as a stochastic mechanism for cell fate determination. This intriguing model also conveniently explains the reduced size of affected tissues in the heterozygous mutants.

Heterozygous mutations in *Pax6* are responsible for the Small eye (Sey) phenotype in the mouse, and aniridia and Peters' Anomaly in humans (Hill et al., 1991; Ton et al., 1991; Hanson et al., 1994). The Small eye mouse is a valuable animal model for these diseases (Jordan et al., 1992; Hanson et al., 1994). Overlapping defects include iris hypoplasia, adhesions between the lens and the cornea, and corneal opacification.

Eye development in mice begins at embryonic day (E) 8.0 when the optic vesicle forms from pits in the forebrain and grows towards the surface of the head (Fig. 1). The head ectoderm is biased toward lens formation, and when it comes into close apposition to the optic vesicle, it is induced to form the lens placode, a group of thickened, columnar cells. The lens placode invaginates to form a cup and pinches off from the

surface coordinately with the collapse of the optic vesicle into the two-layered retina (Piatigorsky, 1981; Grainger et al., 1997).

Homozygous *Pax6* mutants fail to form a lens placode (Grindley et al., 1995). Although *Pax6* has been shown to be essential for multiple steps in eye formation (Hogan et al., 1986; Grindley et al., 1995; Cvekl and Piatigorsky, 1996; Wawersik et al., 1999; Collinson et al., 2000), we have focused our study on the consequence of *Pax6* haploinsufficiency on lens development. The reason for focusing on the lens comes from studies of chimeric mice composed of wild-type (+/+) and homozygous *Pax6* mutant (–/–) cells. These studies conclusively showed that –/– cells were excluded from the lens-forming pre-placode beginning at E9.5 (Quinn et al., 1996; Collinson et al., 2000), indicating a cell autonomous requirement for *Pax6* in the lens prior to placode formation. Furthermore *Pax6* heterozygotes display a small lens during embryogenesis, indicating that this tissue is sensitive to a 50% reduction in *Pax6* gene dosage (Theiler et al., 1978).

We have found that the consequence of reduced gene dosage of *Pax6* in heterozygous lenses is first evident as a delay in lens placode formation. After the lens vesicle is formed, the growth rate of the heterozygous lens cells is the same as wild type, but there are 50% fewer cells. This work thus defines a critical stage in lens development that requires wild-type *Pax6* gene dosage. Using two different tests, we show that *Pax6* is biallelically expressed at this critical stage, and therefore monoallelic expression cannot explain the reduced lens size. We propose that the delay in lens development in heterozygotes arises from a delay in achieving a threshold of PAX6 that is required for the correct timing of placode formation and specification of lens cells.

MATERIALS AND METHODS

Animals

The *Pax6* mutant allele, $Pax6^{Sey\text{-}1Neu}$, is a point mutation in the donor splice site junction of the tenth intron (Hill et al., 1991). $Pax6^{Sey\text{-}1Neu}$ mice were a gift from Dr Tom Glaser. Mice carrying the mutation have been maintained on a C3H/HeJ background for at least 9 generations.

Embryo collection and genotyping

Embryos were staged using noon of the day that the plug was detected as E0.5. Where indicated, the number of somites were counted for precise comparison of embryonic developmental stage. *Pax6* alleles were genotyped using DNA prepared from extra-embryonic membranes. The samples were digested for 3 hours at 55°C in 50 μl of 1× PCR Buffer, 0.05% SDS, 0.5 mg/ml Proteinase K. Samples were heat inactivated at 95°C for 15 minutes, chilled at 4°C for 30 minutes, and centrifuged briefly. Each 100 μl PCR reaction contained 2 μl DNA, 6 pmol of each primer, 1× PCR buffer, 0.125 mM dNTPs and 3 Units *Taq* polymerase and were amplified for 35 cycles of 30 seconds at 95°C, 1 minute at 58°C, and 1 minute at 72°C. Primers were (forward) 5′CCAGTGTCTACCAGCCAATC3′ and (reverse) 5′ACTGTACGTGTTGGTGAGGG3′. Portions of the PCR reactions were digested separately with *Hpa*I or *Bst*NI for 3 hours, and analyzed on a 7.5% acrylamide gel. The 220 bp wild-type allele was digested by *Bst*NI, and the $Pax6^{Sey\text{-}1Neu}$ allele was digested by *Hpa*I.

Embedding and histology

For paraffin wax embedding, samples were fixed in either methanol (SOX2) or 4% paraformaldehyde (lens cell number assay, N-cadherin and in situ hybridization) in phosphate buffered saline (PBS) overnight at 4°C. Samples were washed in PBS (unless otherwise stated, all washes were in PBS). The samples were dehydrated through an ethanol/H_2O series, and washed with 100% xylene, 50% xylene/50% Paraplast Plus paraffin (Oxford), and 100% paraffin before embedding. 11 μm sections were obtained and dried. Slides were mounted with either GVA (Zymed) or Vectashield (Vector). For cryosectioning of samples (mitotic index and TUNEL), embryos were fixed overnight in 4% paraformaldehyde at 4ºC. Samples were then washed with sucrose and embedded in OCT (Sakura).

Lens cell number assay

Lenses were serially sectioned, and every section containing lens was examined. Sections were dewaxed, rehydrated, washed and mounted in Vectashield containing 0.01 μg/ml DAPI to stain the nuclei. Images were obtained using fluorescence microscopy and a CCD camera, and analyzed using the imaging software, Metamorph. Regions containing lens nuclei were traced, and the area within the traced region was calculated by Metamorph in relative area units and summed for all areas for a given lens. Using this total, the number of nuclei per lens was calculated from measurements of the density of nuclei in the lens. Error in the calculation of the average lens cell number was determined by calculating the standard error of the mean.

TUNEL assay

Sections were fixed in 4% paraformaldehyde for 20 minutes at room temperature, and washed. Sections were then incubated in permeabilisation solution (0.1% Triton X-100 in 0.1% sodium citrate) for 2 minutes on ice, and rinsed twice. TUNEL reaction mixture (fluorescein label; Boehringer Mannheim) was incubated on each slide for 1 hour at 37°C. Sections were washed, mounted with DAPI, and viewed by fluorescence microscopy. A negative (TUNEL reaction mixture lacking TdT) control was included in each experiment.

Immunohistochemistry

For mitotic index, lens sections were washed and blocked for 1 hour at room temperature in 8% BSA in PBS. Slides were washed and incubated overnight at 4°C with 5 μg/ml anti-phospho-histone H3 (Upstate) in 1% BSA in PBS. Slides were washed and incubated with 20 μg/ml anti-rabbit IgG fluorescein-conjugated antibody (Vector) in 1% BSA in PBS for 1 hour at room temperature. Slides were washed and mounted with DAPI. The mitotic index is the number of positively stained nuclei divided by the estimated number of nuclei, averaged for data from at least 4 lenses. The error was calculated by the standard error of the mean. A negative control (no primary antibody) was included with each experiment and showed no specific signal.

For SOX2 immunohistochemistry, sections were blocked for 1 hour at room temperature in 10% sheep serum in PBS with 0.2% Tween 20. Sections were then incubated overnight at 4°C in a 1:500 dilution of anti-SOX2 antibody (a gift from Dr Robin Lovell-Badge) in blocking solution. Slides were washed, then incubated with 20 μg/ml goat anti-rabbit IgG fluorescein-conjugated antibody (Vector) in blocking solution for 1 hour at room temperature. Slides were washed, mounted with DAPI and analyzed by fluorescence microscopy. A negative control (no primary antibody) was included with each experiment, and showed no specific signal.

For N-cadherin, slides were boiled for 10 minutes in 0.01 M citrate buffer pH 6, and cooled. Slides were washed and blocked in 10 ml PBS containing 1% BSA and 100 μl of sheep serum at room temperature for 1 hour. Slides were incubated with 1:500 dilution of anti-N-cadherin antibody (Zymed 33-3900) in blocking solution overnight at 4°C, washed, and incubated with 1:10 dilution of anti-mouse-IgG antibody conjugated to fluorescein (Jackson Immuno Research) in 1% BSA for 1 hour at room temperature. Slides were washed, mounted with DAPI, and analyzed by fluorescence microscopy. Negative controls showed autofluorescent nuclei in these

paraformaldehyde-fixed, paraffin-embedded sections (see Fig. 5), easily distinguished from actual cell surface staining.

In situ hybridization

In situ hybridization was performed on tissue sections and whole mounts, as described by Wilkinson and Nieto (1993). During whole-mount hybridization, embryos were incubated overnight at 56ºC in hybridization buffer containing 0.6 μg/ml digoxigenin-labeled in vitro-transcribed antisense RNA derived from full-length *Pax6* cDNA (a gift from Dr Peter Gruss; Walther and Gruss, 1991). For in situ hybridization on sections, samples were hybridized overnight at 70°C with 0.1 μg/100 μl of digoxigenin-labeled in vitro-transcribed probe. The $Pax6^{Sey\text{-}1Neu}$ specific probe contained 93 nucleotides of intron 10. The non-allele-specific 3′UTR probe was 186 nucleotides long within exon 13.

RNA-DNA FISH

Fluorescence in situ hybridization (FISH) was carried out as described by Johnson et al. (1991). Neural retinas from E12.5 embryos were dissected, pooled, and dissociated into single cell layers by pipetting in 1× trypsin-EDTA for 3 minutes at 25°C. Cells were spun onto slides using Cytofunnels (Shandon). E10 eyes were dissected, pooled and shredded into very small fragments directly on Superfrost Plus slides (Fisher) using forceps. These slides were air dried. Slides were quickly rinsed, and then were washed in cytoskeletal buffer (CB: 100 mM NaCl, 300 mM sucrose, 3 mM $MgCl_2$, 10 mM Pipes pH 6.8), CB plus 0.5% Triton X-100, and CB for 30 seconds each step. Slides were then fixed in 4% paraformaldehyde for 10 minutes and stored in 70% ethanol at 4°C. For RNA FISH, slides were dehydrated and hybridized overnight at 37°C with biotin-labeled exons 2-13 of *Pax6* genomic DNA (approx. 20 kb) in Hybrisol VII (Oncor) with Cot-1 and salmon sperm DNA. Slides were washed in 50% formamide, 2× SSC at 39°C for 3× 5 minutes, 2× SSC at 39°C for 3× 5 minutes, 1× SSC for 10 minutes, and 4× SSC for 5 minutes. Biotin was detected with FITC-avidin and anti-avidin D (Vector). Avidin was post-fixed for 10 minutes in 4% paraformaldehyde. For subsequent DNA FISH, slides were treated with RNase and washed with 70% formamide, 2× SSC at 70°C for 2 minutes. Slides were hybridized as above to rhodamine-labeled BAC 255020, which contains approx. 150 kb of genomic DNA including the entire *Pax6* gene. Slides were washed as above. Total DNA was visualized with DAPI. Fluorescent signal was analyzed with microscopy (Nikon Eclipse E800) and photographed with a CCD camera. Images were merged using Metamorph imaging software.

RESULTS

Temporal reduction in lens cell number in *Pax6* heterozygotes

Theiler et al. (1978) observed that $Pax6^{+/-}$ embryonic lenses are smaller than wild type. To determine the cause of this reduction, we used $Pax6^{Sey\text{-}1Neu}$/+ heterozygous animals that have a point mutation in a splice junction and produce a truncated protein missing the activation domain of PAX6. This allele is thought to be a null allele, based on the observation that the adult small eye phenotype of $Pax6^{Sey\text{-}1Neu}$/+ mice is identical to mice heterozygous for $Pax6^{Sey\text{-}Dey}$ and $Pax6^{Sey\text{-}H}$, two deletions of *Pax6*. As will be shown below, the small embryonic lens and delay in lens development first described in $Pax6^{Sey\text{-}Dey}$ embryos were also found in $Pax6^{Sey\text{-}1Neu}$ embryos (Theiler et al., 1978; Glaser et al., 1990; Hill et al., 1991).

We serially sectioned wild-type and $Pax6^{Sey\text{-}1Neu}$/+ eyes, and calculated the number of cells in each lens (Fig. 2). While we found no differences in the overall densities of nuclei in the lens at each time point examined (data not shown), we observed on average 49±5% fewer cells in $Pax6^{Sey\text{-}1Neu}$/+ lenses than wild-type lenses at E10.5. This difference was maintained at E11.5 (56±6%) and E12.5 (46±3%). From this we conclude that the reduction in the size of the lens is due to a reduced number of lens cells, and that the reduction occurs prior to E10.5. After E10.5, the growth rate of the lens was identical in heterozygotes and wild-type animals. Furthermore, $Pax6^{Sey\text{-}1Neu}$/+ lenses are no more variable in size between animals than wild-type lenses, implying that the reduction in *Pax6* gene function is affecting animals in a consistent manner.

We then analyzed 24-somite stage wild-type and $Pax6^{Sey\text{-}1Neu}$/+ pre-placode surface ectoderm by determining the number of nuclei in direct contact with the optic vesicle, with no intervening mesenchymal cells. These are the cells that will give rise to the lens placode (Furuta and Hogan, 1998).

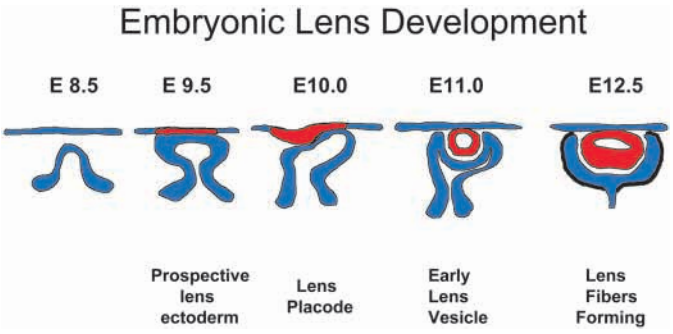

Fig. 1. The development of the lens. The developing lens (red) and retina (blue) between E8.5 and E12.5 are depicted. The pigmented retina is indicated by the thick black line.

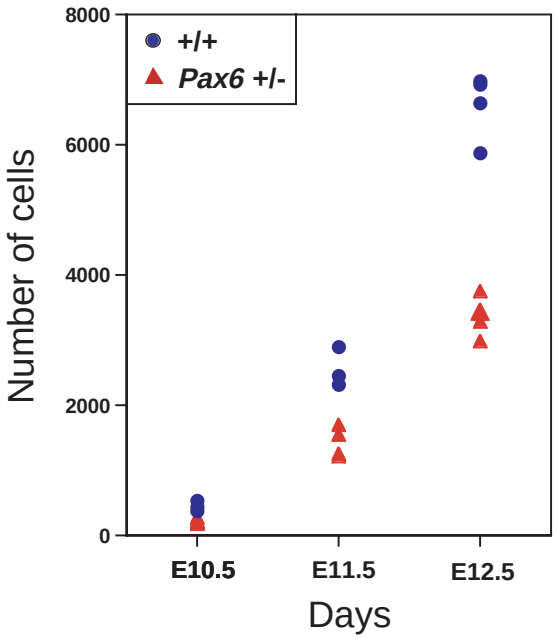

Fig. 2. The number of cells in $Pax6^{Sey\text{-}1Neu}$/+ and wild-type lenses. The number of cells in wild-type (blue circles) and heterozygous *Pax6* mutant (red triangles) lenses is shown. Each point represents the number of cells in a single lens.

We found that there was no significant difference in the average number of cells in wild-type and *Pax6*$^{Sey\text{-}1Neu}$/+ embryos (317±32 and 303±24, respectively). Thus the reduction in lens cell number in *Pax6*$^{Sey\text{-}1Neu}$/+ embryos appears to occur between E9.75 and E10.5, at the time of lens placode formation. Furthermore no differences were noted in the extent or degree of contact between the *Pax6*$^{Sey\text{-}1Neu}$/+ distal optic vesicle and the pre-placode.

Mitotic index developing lenses

To determine what is responsible for the cell number reduction, we measured the rate of mitosis in the lens at stages between E9.75 and E10.5 in wild-type and *Pax6*$^{Sey\text{-}1Neu}$/+ embryos using an antibody specific to phosphorylated histone H3, a marker of mitosis (Hendzel et al., 1997; Fig. 3). We detected no significant difference in the mitotic index in the pre-placode surface ectoderm nuclei that were in direct contact with the optic vesicle in E9.75 wild-type and *Pax6*$^{Sey\text{-}1Neu}$/+ embryos (4.0±1.3% and 4.0±0.6%, respectively; Fig. 3A,B). Likewise at E10.25, when the lens placode had not yet finished its invagination to form the lens vesicle (Fig. 3C,D), no significant difference in the mitotic index in wild-type and *Pax6*$^{Sey\text{-}1Neu}$/+ placodes was detected (4.3±0.6% and 4.0±0.3%, respectively). Thus differences in the mitotic index cannot account for the decrease in lens cells observed between E9.75 and E10.5. These data also show that there is no increase in proliferation after placode formation.

By E12.5, the lens has differentiated into the anterior epithelial layer (e in Fig. 3E,F) and the lens fiber compartment (f). At E12.5, primary lens fibers have exited the cell cycle and are in the process of enucleation. The epithelial layer continues to proliferate and gradually supplies new fiber cells (Piatigorsky, 1981). In wild-type and *Pax6*$^{Sey\text{-}1Neu}$/+ E12.5 lenses, we observed no mitotic cells in the lens fiber compartment, indicating that the *Pax6*$^{Sey\text{-}1Neu}$/+ fiber cells exit the cell cycle normally. At the same time, there were on average 46±3% fewer cells in the *Pax6*$^{Sey\text{-}1Neu}$/+ lens as compared to wild type (Fig. 2). Together, this indicates that *Pax6*$^{Sey\text{-}1Neu}$/+ primary fiber cells do not continue to proliferate longer than wild-type cells and therefore cannot 'catch-up' in number with wild type after E12.5.

Apoptosis in the developing lenses

Increased apoptosis has been suggested to be the underlying cause of the *Pax* gene haploinsufficiency, based on the finding of a *Pax* consensus site in the promoter region of the *p53* gene. It was proposed that a decrease in PAX protein could cause a relaxation in the negative regulation of *p53* and lead to aberrant apoptosis and a reduction in the tissues (Stuart et al., 1995). Recently, increased apoptosis was found to be correlated with reduced *Pax2* gene dosage in the kidney (Ostrom et al., 2000).

Using the TUNEL assay, we observed no difference in the amount of apoptosis in E9.75 wild-type and *Pax6*$^{Sey\text{-}1Neu}$/+ pre-placode surface ectoderm; indeed there were almost no TUNEL-positive nuclei present in either sample (Fig. 4A,B). After placode formation, TUNEL-positive nuclei were present at the edges of the wild-type placode, where the placode connects with the rest of the surface ectoderm (see arrows in Fig. 4C,E). This ring of cell death around the lens cup has been documented for several vertebrates, and is likely required for the separation of the lens vesicle from the surface (Weil et al., 1997; Silver and Hughes, 1973). We did not observe these TUNEL-positive cells in similarly staged *Pax6*$^{Sey\text{-}1Neu}$/+ embryos at either the placode (E10.0) or the lens cup (E10.25) stage (arrows in Fig. 4D,F), and found no increased apoptosis in the body of the placode or cup. Therefore, increased apoptosis is not the cause of the lens cell number reduction in *Pax6*$^{Sey\text{-}1Neu}$/+ embryos between E9.75 and E10.5.

Temporal formation of the lens placode

It was reported in a study of *Pax6*$^{Sey\text{-}Dey}$ mice that some of the

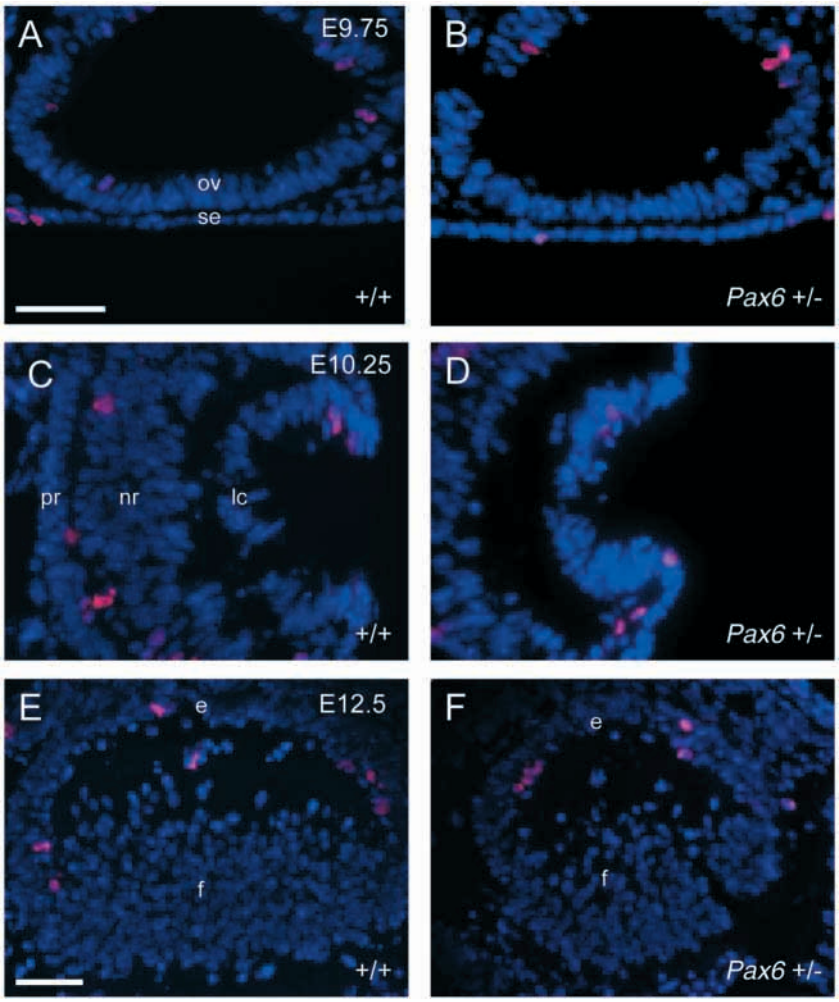

Fig. 3. The number of dividing cells in *Pax6*$^{Sey\text{-}1Neu}$/+ and wild-type lenses. Anti-phospho-histone H3 antibody (red) and DAPI staining (blue) of *Pax6* wild-type (A,C,E) or *Pax6*$^{Sey\text{-}1Neu}$/+ (B,D,F) lens sections at the days indicated. The scale bar in A and E represents 50 μm. Surface ectoderm, se; optic vesicle, ov; pigmented retina, pr; neural retina, nr; lens cup, lc; epithelial layer, e; lens fibers, f. The number of cells examined were 822 (A), 670 (B), 4291 (C), 1520 (D).

embryos from heterozygous intercrosses had not developed lens pits at E10.0 (Theiler et al., 1978). However, it was not clear whether this was a general delay, or a delay specifically in lens development. To investigate this, we collected embryos with 25, 26 and 27 somites, serially sectioned the eyes, and stained with hematoxylin. In this pool, the average somite number for wild-type embryos was 26.2 and for *Pax6*$^{Sey\text{-}1Neu}$/+ embryos was 26.0 (Table 1). We found that 89.5% of wild-type embryos but only 60.0% of *Pax6*$^{Sey\text{-}1Neu}$/+ embryos had developed placodes, a statistically significant difference (P<0.005; χ^2 analysis). Thus the *Pax6*$^{Sey\text{-}1Neu}$/+ small lens phenotype can first be detected as a delay in placode formation, and does not reflect a general developmental delay in *Pax6*$^{Sey\text{-}1Neu}$/+ animals.

Table 1. Placode development in wild-type and *Pax6*$^{Sey\text{-}1Neu}$/+ embryos

Number of somites	Number of embryos with placodes	
	Wild type	*Pax6*$^{Sey\text{-}1Neu}$/+
25	4/4	4/6
26	6/8	0/3
27	7/7	5/6
Total	17/19	9/15

Embryos were examined for placode development prior to genotyping, based on the appearance of thickened columnar patches of cells revealed by hematoxylin staining.

Expression of N-cadherin in the developing lens

The formation of the lens placode is characterized by changes in both cell shape and nuclei elongation. To better understand these events, and their sensitivity to *Pax6* dosage, we examined the expression of N-cadherin, a calcium-dependent cell adhesion molecule that is associated with the separation and sealing of cell layers in morphogenesis. As lens placode cells form, they begin to express N-cadherin, while surrounding epithelial cells continue to express only E-cadherin (Takeichi, 1988). Regulation of R-cadherin expression in the brain by *Pax6* has been reported (Stoykova et al., 1997).

We detected high levels of N-cadherin in the optic cup and lower levels in the outer surface of the wild-type lens placode at the 27-somite stage (Fig. 5A). At the 29- and 32-somite stage, the amount of N-cadherin increases in the wild-type lens (Fig. 5C,E), similar to reported studies in chicks (Hatta and Takeichi, 1986). A comparable increase in N-cadherin was not seen in the *Pax6*$^{Sey\text{-}1Neu}$/+ lens until the 32-somite stage (Fig. 5F), and it is not until the 34-somite stage that N-cadherin expression reaches levels equal in intensity to that of the 32-somite stage wild-type lens (Fig. 5G). Thus, *Pax6*$^{Sey\text{-}1Neu}$/+ lenses begin to express high levels of N-cadherin protein approx. 3 somite stages later than wild-type lenses. The consistent delay of approx. 3 somites in N-cadherin up-regulation in *Pax6*$^{Sey\text{-}1Neu}$/+ embryos is comparable to the morphological delay that we observed in placode formation (see Table 1) and lens invagination (Fig. 5).

Three additional defects can be observed at this stage in *Pax6*$^{Sey\text{-}1Neu}$/+ lenses. First, the *Pax6*$^{Sey\text{-}1Neu}$/+ embryos have a distinct U-shaped lens cup instead of the C-shape found in wild type (compare Fig. 5F with 5E). Second at the 32- and 34-somite stages, N-cadherin is only detected in the base of the *Pax6*$^{Sey\text{-}1Neu}$/+ lens cup and not in the peripheral region that is adjacent to the surface ectoderm (compare Fig. 5F,G with 5E). Third, this N-cadherin non-expressing region frequently fails to detach from the surface ectoderm and forms a persisting connection between the lens and surface ectoderm known as a lens stalk (Fig. 5G). Aberrant connections between the lens and the cornea in adult eyes are called adhesions, and have been previously observed in *Pax6*^{Sey}/+ mice and human Peters' Anomaly patients. Using in situ hybridization, we found that the *Pax6*$^{Sey\text{-}1Neu}$/+ lens stalk expresses high levels of *Pax6* mRNA at E11.5 (see Fig. 7F). This expression was stronger than in the rest of the lens, suggesting that if the stalk is composed of lens cells, they are less differentiated than the developing lens fibers. We speculate that the failure of the peripheral lens cup cells to undergo normal programmed cell death and to express N-cadherin may contribute to the inability of the *Pax6*$^{Sey\text{-}1Neu}$/+ lens to completely separate from the surface.

Expression of *Pax6* and SOX2 in the developing lens

The delay in the formation of the lens placode is the earliest difference that we detect in the development of *Pax6*$^{Sey\text{-}1Neu}$/+

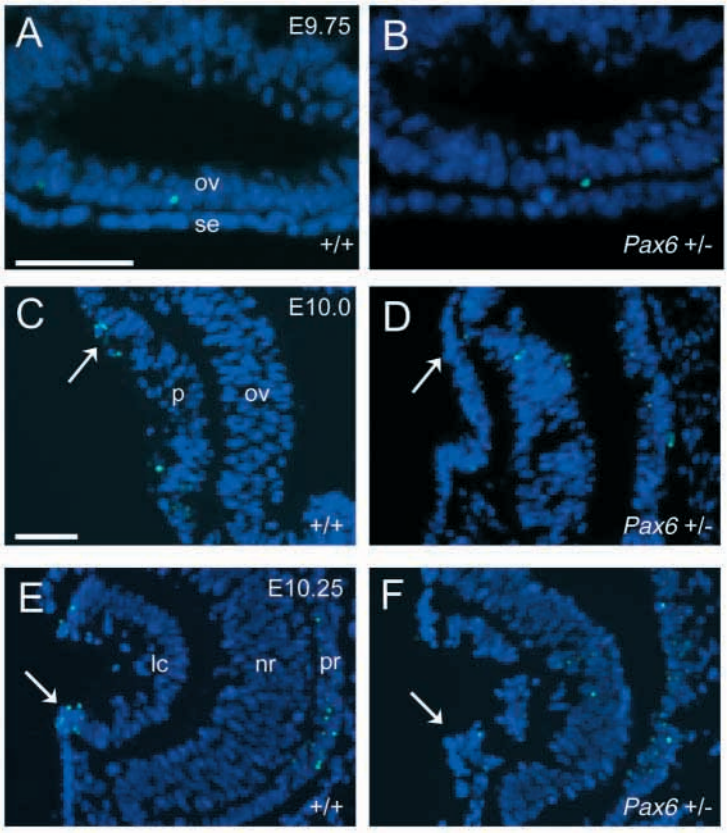

Fig. 4. Apoptosis in *Pax6*$^{Sey\text{-}1Neu}$/+ and wild-type lenses. TUNEL assays were performed on wild-type (A,C,E) and *Pax6*$^{Sey\text{-}1Neu}$/+ (B,D,F) lenses at the days indicated. At E10.0 and E10.25, apoptosis was seen at either edge of lens placode or lens cup in wild-type embryos, but was absent in *Pax6*$^{Sey\text{-}1Neu}$/+ embryos (white arrows). At E10.25, apoptosis is seen in the pigmented epithium. Scale bars in A and C represent 50 μm. Optic vesicle, ov; surface ectoderm, se; lens placode, p; lens cup, lc; pigmented retina, pr; neural retina, nr.

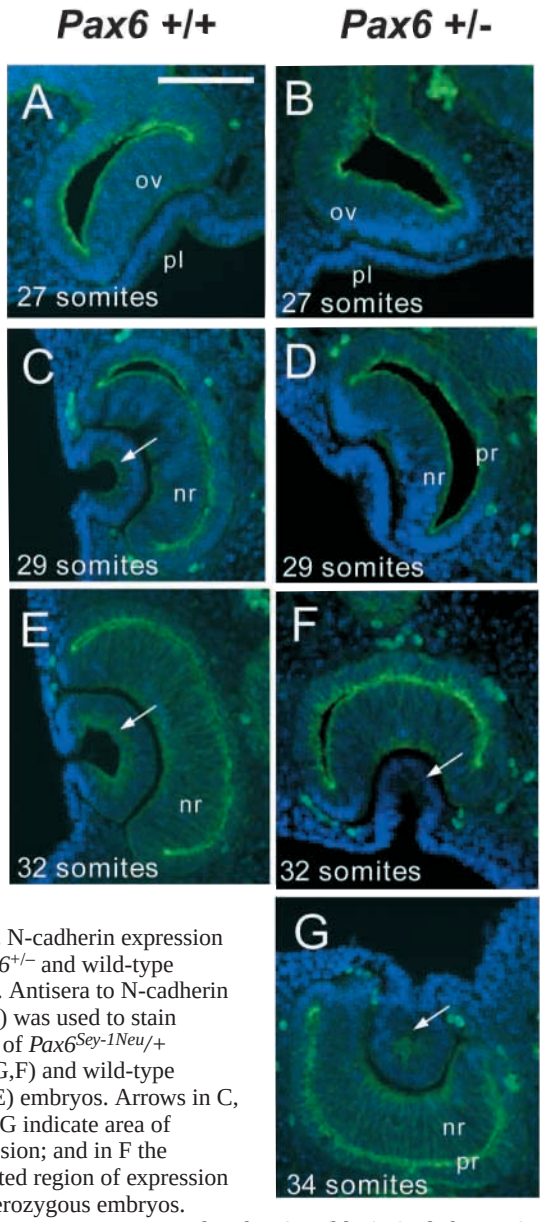

Fig. 5. N-cadherin expression in *Pax6*$^{+/-}$ and wild-type lenses. Antisera to N-cadherin (green) was used to stain lenses of *Pax6*$^{Sey\text{-}1Neu}$/+ (B,D,G,F) and wild-type (A,C,E) embryos. Arrows in C, E and G indicate area of expression; and in F the restricted region of expression in heterozygous embryos. Sections are counter-stained with DAPI (blue). Scale bar in A represents 100 μm. Lens placode, lp; optic vesicle, ov; neural retina, nr; pigmented retina, pr.

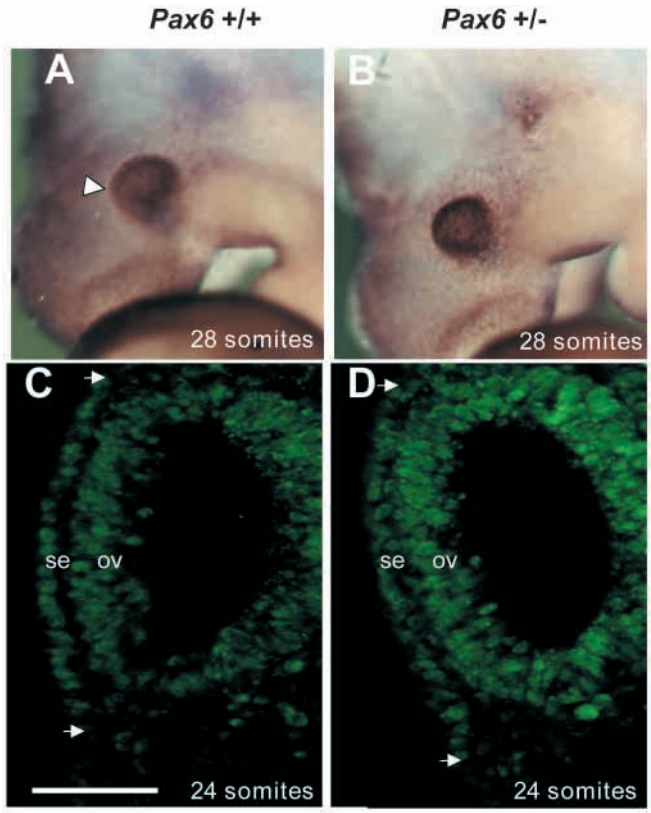

Fig. 6. *Pax6* and SOX2 expression in *Pax6*$^{Sey\text{-}1Neu}$/+ and wild-type embryos. (A,B) Whole-mount in situ hybridization was performed on 28-somite stage wild-type (A) and *Pax6*$^{Sey\text{-}1Neu}$/+ (B) embryos using an antisense *Pax6* probe. The arrowhead in A indicates the developing eye. (C,D) Anti-SOX2 staining (green) of 24 somite stage wild-type (C) and *Pax6*$^{Sey\text{-}1Neu}$/+ (D) embryos. The arrows indicate the boundary of the surface ectoderm nuclei expressing SOX2. Surface ectoderm, se; Optic vesicle, ov. The scale bar in C represents 50 μm.

lenses. To determine whether aspects of early pre-placode lens development are affected in *Pax6*$^{Sey\text{-}1Neu}$/+ embryos, we examined two early markers of lens development, *Pax6* and SOX2. *Pax6* is initially expressed in a broad region of head surface ectoderm covering the prosencephalon at E8.0. Over the next 36 hours, expression becomes restricted to the region overlying the optic vesicle, the lens pre-placode. *Pax6* is possibly required for the maintenance of its own expression in the lens pre-placode, since *Pax6* expression is lost in the head ectoderm of *Pax6*$^{-/-}$ mice by E9.5-9.75 (see Fig. 8E and Grindley et al., 1995). Using an in situ hybridization probe that detects both the wild-type and mutant alleles, we found that *Pax6* was highly expressed in the area of contact between the surface and optic vesicle in both wild-type and *Pax6*$^{Sey\text{-}1Neu}$/+ littermates at 24- and 28-somite stages (Fig. 6A,B and data not shown).

We next examined the expression of SOX2 using anti-SOX2 antisera. SOX2 is an HMG-containing transcription factor that is expressed in the brain and optic vesicle, and in the surface ectoderm beginning at approximately the 18-somite stage (E9.0) (Kamachi et al., 1998). Its expression in the surface ectoderm is dependent upon *Pax6*, as it is not expressed in *Pax6* homozygous mutants (Furuta and Hogan, 1998). The protein is significantly upregulated at the 23- to 24-somite stage and continues to be expressed until SOX1 replaces it at E11.0 (Nishiguchi et al., 1998; Furuta and Hogan, 1998).

When we compared 24 somite wild-type and *Pax6*$^{Sey\text{-}1Neu}$/+ embryos, we found that wild-type and *Pax6*$^{Sey\text{-}1Neu}$/+ embryos expressed high levels of SOX2 in a similar domain in the pre-placode ectoderm (Fig. 6C,D). This region included the nuclei in direct contact with the optic vesicle plus a slight tail of expressing nuclei to one side of the optic vesicle (see region bordered by arrows in Fig. 6). Thus the pre-placode ectoderm is not reduced in size in *Pax6*$^{Sey\text{-}1Neu}$/+ embryos, consistent with our estimate of pre-placode cell number.

The expression of *Pax6* is biallelic

It was recently reported that another member of the *Pax* gene family, *Pax5* (BSAP), is expressed in a stochastic and monoallelic

fashion during pro-B cell development (Nutt et al., 1999). The authors proposed that monoallelic expression could explain the semi-dominant phenotypes seen in many *Pax* genes (Nutt and Busslinger, 1999). That is, heterozygotes would produce functionally normal cells that had activated only the wild-type allele, as well as functionally null cells that had activated only the mutant allele. The latter cells would then fail to specify their fate correctly, thus explaining why *Pax* heterozygotes often display a reduction in the size of affected tissues. Applying this reasoning to *Pax6*, 50% of lens pre-placode cells would activate only the mutant allele, and would fail to become part of the lens. If the transcriptional state of each *Pax6* allele were heritable such that each lens cell and all its descendants maintained expression of the same allele, then no mutant allele-expressing cells should be present in the $Pax6^{Sey\text{-}1Neu}$/+ lens. This prediction follows from the finding that there is a cell autonomous requirement for *Pax6* in the lens-forming surface ectoderm, beginning before E9.5 (Collinson et al., 2000).

We created an in situ hybridization probe within the unspliced 10th intron, which detects the $Pax6^{Sey\text{-}1Neu}$ transcript, but not the wild-type transcript. We used this probe, as well as one derived from the 3′UTR that hybridizes to both the mutant and wild-type transcripts to examine allelic expression in wild type, $Pax6^{Sey\text{-}1Neu}$/+, and $Pax6^{Sey\text{-}1Neu}$/$Pax6^{Sey\text{-}1Neu}$ embryos at E10.5. As expected, the $Pax6^{Sey\text{-}1Neu}$-specific probe did not hybridize to the wild-type lens or optic vesicle (Fig. 7B), and the 3′UTR probe hybridized to the lens and optic vesicle of both the wild type and heterozygous embryos (Fig. 7A,C). As shown in Fig. 7D, we found that the $Pax6^{Sey\text{-}1Neu}$-specific probe hybridized to the $Pax6^{Sey\text{-}1Neu}$/+ lens, indicating that the expression of *Pax6* in the lens is not strictly monoallelic. As an additional control for the efficacy of the $Pax6^{Sey\text{-}1Neu}$ probe, we also examined its hybridization to $Pax6^{Sey\text{-}1Neu}$/$Pax6^{Sey\text{-}1Neu}$ homozygous optic vesicles. As expected, hybridization was strong in the optic vesicle, but not in the overlying ectoderm in which *Pax6* is auto-regulated (Fig. 7E).

This experiment rules out strict monoallelic expression of *Pax6* in which only one allele of *Pax6* is expressed in a lens cell and all its descendants. However, *Pax6* expression could switch between the two alleles, or the gene could be activated in a stochastic manner such that only some cells express both alleles, as has been observed for *Pax5* expression (Nutt et al., 1999). To test these possibilities for *Pax6*, we examined the expression of *Pax6* in single cells using RNA-DNA fluorescence in situ hybridization (FISH) analysis (Johnson et al., 1991). Wild-type neural retinas at E12.5 were dissected, pooled, dissociated and the cells were immediately spun onto slides. Whole wild-type E10 eyes were dissected, pooled, and shredded into fragments on slides. A few cells from many different patches were examined to ensure a random sampling of this mix of lens placode and optic cup cells. Nascent *Pax6* RNA was detected using a DNA probe specific to exons 2-13 of *Pax6* genomic DNA. The *Pax6* alleles were subsequently detected with DNA FISH (Fig. 8). By examining only those cells that displayed two DNA signals, we limited our analysis to cells in which both alleles had access to the hybridization probes. In that population, the RNA probe hybridized to 98% of cells from the neural retina and 82% of cells from the E10 eye. In the *Pax6*-expressing cells, RNA was detected at both *Pax6* loci in 88% of neural retina cells and 93% of E10 eye cells (n=50, n=55, respectively). Thus in the majority of cells, *Pax6* RNA was biallelically expressed. No *Pax6* RNA was detected in E10 limb bud cells (Fig. 8H) or in neural retinal cells treated with RNase before RNA FISH (Fig. 8G). Thus at the time when the reduction in lens cell number occurs in $Pax6^{Sey\text{-}1Neu}$/+ embryos, *Pax6* is almost entirely biallelically expressed. Therefore monoallelic expression cannot account for the haplo-insufficient small lens phenotype of *Pax6*.

DISCUSSION

Reduction in *Pax6* gene dosage is deleterious during lens placode formation

The purpose of this study was to understand the basis for the

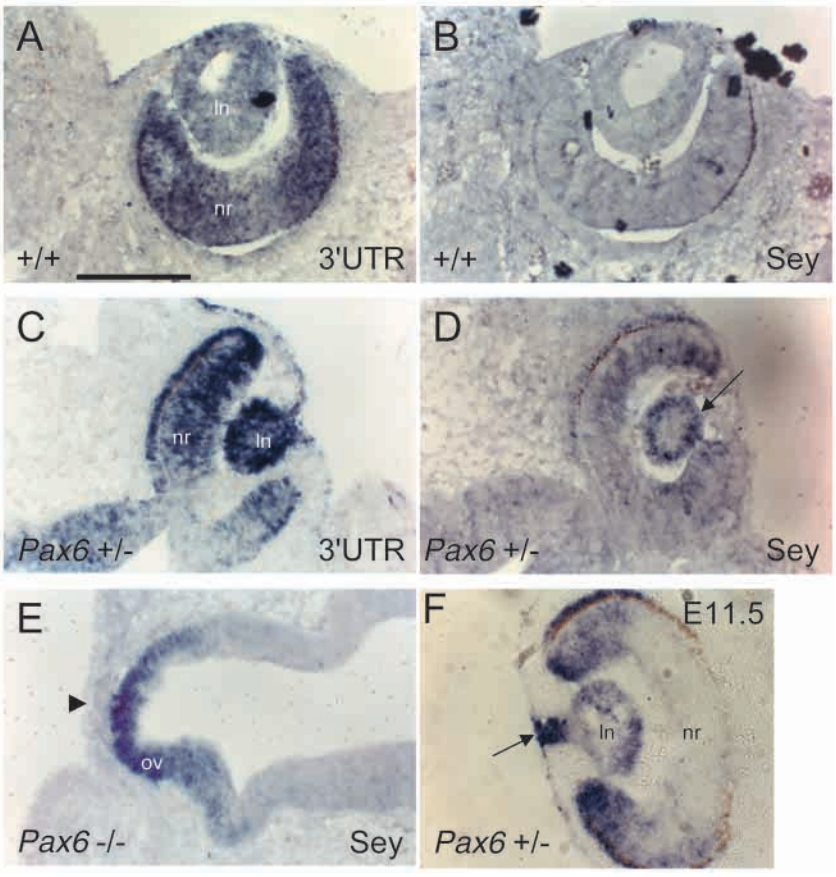

Fig. 7. *Pax6* is not strictly monoallelically expressed. E10.5 wild type (A,B), $Pax6^{Sey\text{-}1Neu}$/+ (C,D), and $Pax6^{Sey\text{-}1Neu}$/ $Pax6^{Sey\text{-}1Neu}$(E) lens sections were hybridized to either a 3′UTR probe (A,C) or an intron 10 probe (Sey; B,D, and E). The arrow in D indicates the lens. The arrowhead in E indicates the surface ectoderm lacking *Pax6* expression. (F) E11.5 $Pax6^{Sey\text{-}1Neu}$/+ lens section with lens stalk (arrow) hybridized to the 3′UTR probe. The scale bar in A represents 200 μm. Lens, ln; neural retina, nr; optic vesicle, ov.

haplo-insufficient small lens phenotype of *Pax6*$^{+/-}$ mice. Our findings suggest that the 50% reduction in *Pax6* gene dosage in heterozygotes is deleterious between E9.75 and E10.5, around the time when the lens placode is induced and the lens cup is forming. Before and after this point, lens development appears to be normal, even though *Pax6* is required for pre-placode development.

The 50% reduction in lens cell number was a strikingly consistent finding from animal to animal, and suggested a regulated mechanism. We tested whether the 50% reduction was caused by monoallelic expression of *Pax6* in the pre-placode. Using two independent methods, we demonstrated that *Pax6* is biallelically expressed in the majority of cells in the lens. This result is in contrast to that of Nutt et al. (1999) who found that *Pax5* was stochastically activated in a monoallelic fashion in B cells. However *Pax5* monoallelism has recently been challenged by Rhoades et al. (2000). Thus allelic exclusion does not explain all semi-dominant phenotypes of *Pax* genes.

The 50% reduction in lens cell number in *Pax6*$^{Sey\text{-}1Neu}$/+ embryos is best explained by a delay in lens placode formation. In this model, heterozygous placode cells, the precursors of lens cells, are specificied ~3 somite stages later than in wild type, resulting in lens cells with less time to proliferate before terminal differentiation into lens fibers. In support of this, we observed a smaller lens at every stage after placode formation, and that the lens cells exited from the cell cycle at the same time as wild-type cells. Thus there was no opportunity for the heterozygous lens to compensate. The consistent 50% reduction in cell number implies that the delay results in *Pax6*$^{Sey\text{-}1Neu}$/+ lens cells missing one round of cell division. It has recently been observed that lacrimal gland development is also delayed in *Pax6*$^{+/-}$ mice (Makarenkova et al., 2000).

The lens placode is sensitive to *Pax6* dosage

The delay in lens placode formation could arise from *Pax6* haplo-insufficiency in the surface ectoderm, in the optic vesicle, or both. However, several lines of evidence support the surface ectoderm. Tissue recombination experiments and *Pax6* chimeric embryos were used to show that there is a direct requirement for *Pax6* in the surface ectoderm for lens placode formation (Fujiwara et al., 1994; Quinn et al., 1996; Collison et al., 2000). In contrast, *Pax6*$^{-/-}$ optic vesicles are able to induce lens placodes in wild-type ectoderm. Therefore, *Pax6* is not required in the optic vesicle to induce the placode. However, the chimera studies revealed a requirement for *Pax6* in the optic vesicle in order for it to make direct contact with the surface ectoderm. Thus *Pax6*$^{-/-}$ optic vesicles were less efficient at placode formation because they were often not in direct contact with the ectoderm. In our studies of heterozygous embryos, we did not detect any difference in the contact of the pre-placode surface ectoderm with the optic vesicle (see Figs 3B, 4B, 6B as examples). Thus the heterozygous optic vesicles were in the correct juxtaposition for placode formation.

SOX2 is a marker for the response of the ectoderm to the inductive signal of the optic vesicle. For example, in tissue recombination experiments, SOX2 up-regulation in the ectoderm only occurred in the presence of BMP4, a secreted signaling molecule that is a component of the optic vesicle signal (Furuta and Hogan, 1998). The normal expression of SOX2 in *Pax6*$^{Sey\text{-}1Neu}$/+ embryos suggests that the surface ectoderm correctly received the signal sent by the optic vesicle, but was delayed in its ability to respond.

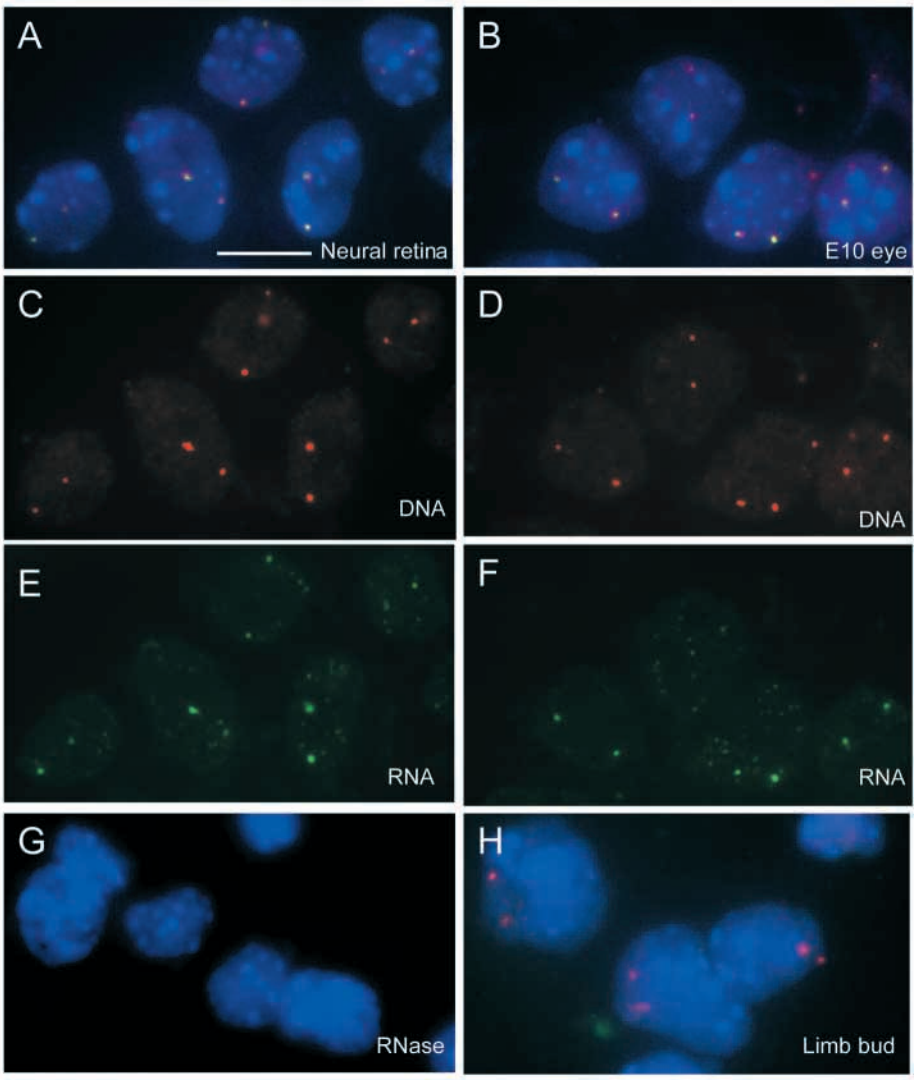

Fig. 8. *Pax6* is biallelically expressed in most cells. RNA-DNA FISH analysis of *Pax6* expression in E12.5 neural retina cells (A,C,E) and E10 eye cells (B,D,F). RNA, green; DNA, red; DAPI, blue. (C,D) DNA signal. (E,F) RNA signal. (G) No *Pax6* RNA is detected by RNA FISH in E12.5 neural retinal cells after RNase treatment. (H) *Pax6* RNA is not detected by RNA-DNA FISH in limb bud cells. The scale bar in A represents 10 μm.

A threshold model for *Pax6* haplo-insufficiency in the lens

We propose that lens placode formation requires the activation of a set of genes that are particularly sensitive to the concentration of PAX6. As *Pax6*$^{Sey\text{-}1Neu}$/+ cells will take longer to reach a threshold of PAX6, it follows that lens placode formation will be delayed. The fact that the expression of *Pax6* is gradually upregulated in the future placode, coupled with the possibility that *Pax6* is autoregulated in the placode, suggests that there may be tight control over the timing of acquisition of the critical threshold level. It will be important to determine whether autoregulation is a component of dosage sensitivity, as *Pax6* is not autoregulated in all tissues, for example in the optic vesicle (see Fig. 7E). Different thresholds for PAX6 action could be part of the mechanism by which *Pax6* controls specific cell fate decisions despite its expression in virtually all of the structures of the developing eye (Grindley et al., 1995).

We noticed that the cells at the edge of *Pax6*$^{Sey\text{-}1Neu}$/+ lens cups do not express N-cadherin and do not undergo normal apoptosis. This suggests that PAX6 may be required at a specific level at the right time to specify a unique fate for these cells and create a sharp boundary between these cells and the rest of the ectoderm. This specification apparently does not occur, since the lens vesicle fails to completely separate. These aspects of the *Pax6*$^{+/-}$ phenotype are reminiscent of transcription factor gradients in *Drosophila*, such as Hunchback and Dorsal, which are required at different threshold amounts to pattern the early embryo (Mannervik et al 1999).

Mammalian haplo-insufficiency

As more mammalian genes are characterized, it is commonly observed that transcription factors are prone to having semi-dominant loss-of-function phenotypes (Herrmann et al., 1990; Fisher and Scambler, 1994; Wilkie, 1994; Engelkamp and van Heyningen, 1996). At least some of these transcription factors, for example *Pitx2* (Gage et al., 1999), are required at precise levels to specify cell fate. Generalizing from this study, it may be that some transcription factors are required at very specific levels during relatively short windows of time. Failure to initiate a developmental event in time may lead to defects that cannot be corrected. This appears to be the case for *Pax6*, where the failure to specify the normal number of lens cells in heterozygotes is not compensated for later. It remains to be determined why this dosage sensitivity is so prevalent in mammals, but not in invertebrates. A screen of the *Drosophila* FlyBase (http://flybase.bio.indiana.edu) identified only two genes that displayed semi-dominant loss-of-function phenotypes.

The authors would like to thank Dr Tom Glaser at the University of Michigan for the *Pax6*$^{Sey-1Neu}$ mice, Dr Peter Gruss at the Max-Planck-Institute of Biophysical Chemistry for the *Pax6* cDNA, and Dr Robin Lovell-Badge at the National Institute for Medical Research, London, for the SOX2 antisera. The authors are also grateful to Dr Barbara Panning, now at the University of California, San Francisco, for detailed advice on the RNA FISH technique, and Dr Lisa Sandell at Princeton University for many stimulating discussions. S. M. T. is an Investigator of the Howard Hughes Medical Institute, which supported this work.

REFERENCES

Baldwin, C. T., Hoth, C. F., Amos, J. A., da-Silva, E. O. and Milunsky, A. (1992). An exonic mutation in the HuP2 paired domain gene causes Waardenburg's syndrome. *Nature* **355**, 637-638.

Collinson, J. M., Hill, R. E. and West, J. D. (2000). Different roles for Pax6 in the optic vesicle and facial epithelium mediate early morphogenesis of the murine eye. *Development* **127**, 945-956.

Cvekl, A. and Piatigorsky, J. (1996). Lens development and crystallin gene expression: many roles for Pax-6. *BioEssays* **18**, 621-630.

Dressler, G. R., Wilkinson, J. E., Rothenpieler, U. W., Patterson, L. T., Williams-Simons, L. and Westphal, H. (1993). Deregulation of Pax-2 expression in transgenic mice generates severe kidney abnormalities. *Nature* **362**, 65-67.

Engelkamp, D. and van Heyningen, V. (1996). Transcription factors in disease. *Curr. Opin. Genet. Dev*. **6**, 334-342.

Epstein, D. J., Vekemans, M. and Gros, P. (1991). Splotch (Sp2H), a mutation affecting development of the mouse neural tube, shows a deletion within the paired homeodomain of Pax-3. *Cell* **67**, 767-774.

Fisher, E. and Scambler, P. (1994). Human haploinsufficiency–one for sorrow, two for joy. *Nat. Genet*. **7**, 5-7.

Fujiwara, M., Uchida, T., Osumi-Yamashita, N. and Eto, K. (1994). Uchida rat (rSey): a new mutant rat with craniofacial abnormalities resembling those of the mouse Sey mutant. *Differentiation* **57**, 31-38.

Furuta, Y. and Hogan, B. L. M. (1998). BMP4 is essential for lens induction in the mouse embryo. *Genes. Dev*. **12**, 3764-3775.

Gage, P. J., Suh, H. and Camper, S. A. (1999) Dosage requirement of Pitx2 for development of multiple organs. *Development* **126,** 4643-4651.

Glaser, T., Lane, J. and Housman, D. (1990). A mouse model of the aniridia-Wilms tumor deletion syndrome. *Science* **250**, 823-827.

Grainger, R. M., Mannion, J. E., Cook, T. L., Jr. and Zygar, C. A. (1997). Defining intermediate stages in cell determination: acquisition of a lens-forming bias in head ectoderm during lens determination. *Dev. Genet*. **20**, 246-257.

Grindley, J. C., Davidson, D. R. and Hill, R. E. (1995). The role of Pax-6 in eye and nasal development. *Development* **121**, 1433-1442.

Hanson, I. M., Fletcher, J. M., Jordan, T., Brown, A., Taylor, D., Adams, R. J., Punnett, H. H. and van Heyningen, V. (1994). Mutations at the PAX6 locus are found in heterogeneous anterior segment malformations including Peters' anomaly. *Nat. Genet*. **6**, 168-173.

Hatta, K. and Takeichi, M. (1986). Expression of N-cadherin adhesion molecules associated with early morphogenetic events in chick development. *Nature* **320**, 447-449.

Hendzel, M. J., Wei, Y., Mancini, M. A., Van Hooser, A., Ranalli, T., Brinkley, B. R., Bazett-Jones, D. P. and Allis, C. D. (1997). Mitosis-specific phosphorylation of histone H3 initiates primarily within pericentromeric heterochromatin during G2 and spreads in an ordered fashion coincident with mitotic chromosome condensation. *Chromosoma* **106**, 348-360.

Herrmann, B. G., Labeit, S., Poustka, A., King, T. R. and Lehrach, H. (1990). Cloning of the T gene required in mesoderm formation in the mouse. *Nature* **343**, 617-622.

Hill, R. E., Favor, J., Hogan, B. L., Ton, C. C., Saunders, G. F., Hanson, I. M., Prosser, J., Jordan, T., Hastie, N. D. and van Heyningen, V. (1991). Mouse small eye results from mutations in a paired-like homeobox-containing gene. *Nature* **354**, 522-525.

Hogan, B. L., Horsburgh, G., Cohen, J., Hetherington, C. M., Fisher, G. and Lyon, M. F. (1986). Small eyes (Sey): a homozygous lethal mutation on chromosome 2 which affects the differentiation of both lens and nasal placodes in the mouse. *J. Embryol. Exp. Morphol*. **97**, 95-110.

Johnson, C. V., Singer, R. H. and Lawrence, J. B. (1991). Fluorescent detection of nuclear RNA and DNA: implications for genome organization. *Methods Cell Biol*. **35**, 73-99.

Jordan, T., Hanson, I., Zaletayev, D., Hodgson, S., Prosser, J., Seawright, A., Hastie, N. and van Heyningen, V. (1992). The human PAX6 gene is mutated in two patients with aniridia. *Nat. Genet*. **1**, 328-332.

Kamachi, Y., Uchikawa, M., Collignon, J., Lovell-Badge, R. and Kondoh, H. (1998). Involvement of Sox1, 2 and 3 in the early and subsequent molecular events of lens induction. *Development* **125**, 2521-2532.

Keller, S. A., Jones, J. M., Boyle, A., Barrow, L. L., Killen, P. D., Green, D. G., Kapousta, N. V., Hitchcock, P. F., Swank, R. T. and Meisler, M. H. (1994). Kidney and retinal defects (Krd), a transgene-induced mutation with a deletion of mouse chromosome 19 that includes the Pax2 locus. *Genomics* **23**, 309-320.

Macchia, P. E., Lapi, P., Krude, H., Pirro, M. T., Missero, C., Chiovato, L., Souabni, A., Baserga, M., Tassi, V., Pinchera, A., Fenzi, G., Gruters, A., Busslinger, M. and Di Lauro, R. (1998). PAX8 mutations associated with congenital hypothyroidism caused by thyroid dysgenesis. *Nat. Genet*. **19**, 83-86.

Makarenkova, H. P., Ito, M., Govindarajan, V., Faber, S. C., Sun, L., McMahon, G., Overbeek, P. A. and Lang, R. A. (2000). FGF10 is an inducer and Pax6 a competence factor for lacrimal gland development. *Development* **127,** 2563-2572.

Mannervik, M., Nibu, Y., Zhang, H. and Levine, M. (1999). Transcriptional coregulators in development. *Science* **284,** 606-609.

Mansouri, A., Goudreau, G. and Gruss, P. (1999). Pax genes and their role in organogenesis. *Cancer Res*. **59**, 1707-1710.

Nishiguchi, S., Wood, H., Kondoh, H., Lovell-Badge, R. and Episkopou, V. (1998). Sox1 directly regulates the gamma-crystallin genes and is essential for lens development in mice. *Genes Dev*. **12**, 776-781.

Nutt, S. L. and Busslinger, M. (1999). Monoallelic expression of Pax5: a paradigm for the haploinsufficiency of mammalian Pax genes? *Biol. Chem*. **380**, 601-611.

Nutt, S. L., Vambrie, S., Steinlein, P., Kozmik, Z., Rolink, A., Weith, A. and Busslinger, M. (1999). Independent regulation of the two Pax5 alleles during B-cell development. *Nat. Genet.* **21**, 390-395.

Ostrom, L., Tang, M. J., Gruss, P. and Dressler, G. R. (2000). Reduced Pax2 Gene Dosage Increases Apoptosis and Slows the Progression of Renal Cystic Disease. *Dev. Biol*. **219**, 250-258.

Piatigorsky, J. (1981). Lens differentiation in vertebrates. A review of cellular and molecular features. *Differentiation* **19**, 134-153.

Quinn, J. C., West, J. D. and Hill, R. E. (1996). Multiple functions for Pax6 in mouse eye and nasal development. *Genes Dev*. **10**, 435-446.

Rhoades, K. L., Singh, N., Simon, I., Glidden, B., Cedar, H. and Chess, A. (2000). Allele-specific expression patterns of interleukin-2 and Pax-5 revealed by a sensitive single-cell RT-PCR analysis. *Curr. Biol.* **10**, 789-792.

Sanyanusin, P., Schimmenti, L. A., McNoe, L. A., Ward, T. A., Pierpont, M. E., Sullivan, M. J., Dobyns, W. B. and Eccles, M. R. (1995). Mutation of the PAX2 gene in a family with optic nerve colobomas, renal anomalies and vesicoureteral reflux. *Nat. Genet*. **9**, 358-364.

Schedl, A., Ross, A., Lee, M., Engelkamp, D., Rashbass, P., van Heyningen, V. and Hastie, N. D. (1996). Influence of PAX6 gene dosage on development: overexpression causes severe eye abnormalities. *Cell* **86**, 71-82.

Silver, J. and Hughes, A. F. W. (1973). The role of cell death during morphogenesis of the mammalian eye. *J. Morph.* **140**, 159-170.

Stockton, D. W., Das, P., Goldenberg, M., D'Souza, R. N. and Patel, P. I. (2000). Mutation of PAX9 is associated with oligodontia. *Nat. Genet*. **24**, 18-19.

Stoykova, A., Gotz, M., Gruss, P. and Prince, J. (1997) Pax6-dependent regulation of adhesive patterning, R-cadherin expression and boundary formation in developing forebrain. *Development* **124**, 3765-3777.

Stuart, E. T., Haffner, R., Oren, M. and Gruss, P. (1995). Loss of p53 function through PAX-mediated transcriptional repression. *EMBO J*. **14**, 5638-45.

Takeichi, M. (1988). The cadherins: cell-cell adhesion molecules controlling animal morphogenesis. *Development* **102**, 639-655.

Theiler, K., Varnum, D. S. and Stevens, L. C. (1978). Development of Dickie's small eye, a mutation in the house mouse. *Anat. Embryol. (Berl.)* **155**, 81-86.

Ton, C. C., Hirvonen, H., Miwa, H., Weil, M. M., Monaghan, P., Jordan, T., van Heyningen, V., Hastie, N. D., Meijers-Heijboer, H., Drechsler, M. and et al. (1991). Positional cloning and characterization of a paired box- and homeobox-containing gene from the aniridia region. *Cell* **67**, 1059-1074.

Walther, C. and Gruss, P. (1991). Pax-6, a murine paired box gene, is expressed in the developing CNS. *Development* **113**, 1435-1449.

Wawersik, S., Purcell, P., Rauchman, M., Dudley, A. T., Robertson, E. J. and Maas, R. (1999). BMP7 acts in murine lens placode development. *Dev. Biol*. **207**, 176-188.

Weil, M., Jacobson, M. D. and Raff, M. C. (1997). Is programmed cell death required for neural tube closure? *Curr. Biol.* **7**, 281-284.

Wilkie, A. O. (1994). The molecular basis of genetic dominance. *J. Med. Genet.* **31**, 89-98.

Wilkinson, D. G. and Nieto, M. A. (1993). Detection of messenger RNA by in situ hybridization to tissue sections and whole mounts. *Methods Enzymol*. **225**, 361-373.

Wilm, B., Dahl, E., Peters, H., Balling, R. and Imai, K. (1998). Targeted disruption of Pax1 defines its null phenotype and proves haploinsufficiency. *Proc. Natl. Acad. Sci. USA* **95**, 8692-8697.